Calibration study of a NO_x emission model for natural gas spark-ignition internal combustion engine

Rastislav Toman[1,*]

[1] *CTU in Prague, Faculty of Mechanical Engineering, Department of Automotive, Combustion Engine and Railway Engineering, Technická 4, 166 07 Prague 6, Czech Republic*

Abstract

The current paper presents a calibration study of a NO_x emission model (EngCylNOx) that is available as a part of the GT-Suite 0D/1D /3D multi-physics CAE system simulation software. The NO calculation in the EngCylNOx model uses the extended Zel'dovich mechanism with the three principal reactions governing the NO formation from molecular nitrogen: N_2 and N oxidation and OH reduction, together with their respective reaction rate equations. For the three reaction rate equations, there are five calibration multipliers: three rate multipliers and two activation energy multipliers. Then, the model incorporates also a sixth calibration multiplier to the predicted net rate of NO_x formation.

A genetic algorithm calibrated the EngCylNOx's six calibration multipliers using a full map measurement from a turbocharged natural gas SI engine with a stoichiometric mixture conditions and external EGR ratio variation. The paper provides an evaluation of performance and predictive abilities of the EngCylNOx model applying different calibration procedures and approaches for several engine operation points achieving satisfactory results.

Keywords: NO_x emissions; extended Zel'dovich mechanism; internal combustion engine; spark-ignition; natural gas engine; genetic algorithm

1. Introduction

The study of pollutant emissions and means of their reduction, together with the improvement of the overall efficiency, is of main interest during the development of a modern internal combustion engine (ICE). The after-treatment systems offer the most effective method to fulfil the legislation limits. However, the costs of such systems also encourage to study the original cause of emissions formation by advanced technologies such as new injection strategies, turbocharging systems or external EGR, and to study their emission reduction potentials. Accurate and robust modelling of the emission formation process than minimizes the costs and time demands of the experimental test necessary during the ICE design and control development.

The focus of here presented paper is a calibration study of the nitrogen oxides (NO_x) emission formation model. This study provides results and methods that can be further used for the specific development in diesel engines, as well as in gasoline or natural gas engines.

The NO_x emissions consist of two main elements: nitric dioxide NO_x and nitric oxide NO, with the latter being the predominant one (70-90%) [1].

The principal source of NO is the oxidation of atmospheric nitrogen, with the additional source from the nitrogen-containing compounds in the fuel itself. Many different mechanisms describe the NO formation process, some of them are summed-up in a recent study of Karaky, Mauviot et al. [2]. As they state, the thermal path of NO formation is a main source of NO production and the extended Zel'dovich mechanism is a basic representation of this phenomena. The original Zel'dovich mechanism consisted of two principal reactions. Lavoaie et al. later added a third reaction to form the extended Zel'dovich mechanism (EZM) [1]. Further extensions and modifications led to the formulation of super-extended Zel'dovich mechanism (SEZM) employing 67 reactions and 13 chemical species by Miller et al. [3] in Ford Motor Company. Another study from the same team compared the performance of the EZM and SEZM in different operating conditions. The authors conclude that SEZM is capable of NO production prediction for diluted (fuel-lean end EGR) and fuel-rich conditions in the range of 10% of test data for most operating conditions (BMEP, A/F ratio, EGR, spark timing) except as a function of speed (RPM). On the hand, the EZM can be in error by more than 40% depending on the operating condition [4].

Extended Zel'dovich mechanism renders a base for many other physical and semi-physical NO_x models developed for different purposes, with their performance depending on the specific approach and physical regions in which they apply the chemical kinetic theory [2].

Since the NO_x formation is highly dependent on the formation temperature and the oxygen concentration, many papers focus on the correct temperature calculation, dividing the combustion chamber into distinct physical zones: burned and unburned zone, or even adopting a multi-zone approach.

Hvězda in [5] combined the multi-zone approach with a chemical equilibrium schemes and chemical kinetics, developing a unique method that solves successfully also the reactions with abnormally high reaction rates, which are normally difficult to handle purely by chemical kinetics.

* Author's contact e-mail: Rastislav.Toman@fs.cvut.cz

A NO_x emissions model studied in this paper – EngCylNOx (or *NOx*) uses the extended Zel'dovich mechanism. It is available as a part of the GT-Suite software package [6].
The *NOx* model adds five different calibration multipliers to the basic EZM reaction rate equations together with one overall calibration multiplier to the predicted NO_x formation net rate (total NO formation rate minus the NO dissociation rate).
The addition of these multipliers allows for the EZM calibration for a specific ICE measurement data and further minimization of the EZM dependencies on the operating conditions – as mentioned in [3, 4].

1.1. Main Goals

The main objectives of this paper are:

- First, to calibrate the *NOx* model on the ICE full map obtaining a single set of optimal model parameters;
- Second, to test the predictive capabilities of the *NOx* model.

The additional goals of the paper are following:

- to summarize the main features of the *NOx* model;
- to compare different calibration approaches, with different calibration objective functions.

1.2. Outline of the paper

Section 2 of the paper summarizes the main features of the *NOx* model adopted in this work. Then, section 3 briefly describes the experimental set-up and informs about the test matrix. Following the report on the calibration procedures in section 4, the section 5 sums-up the important results and evaluation of the model's predictive capabilities. The final section 6 contains principal findings and shows prospects for the future work.

2. NO_x emissions model

NOx model uses the three principle reactions (equations 1-3) that primarily control the production of thermal NO, the same way as the other EZM models.

$$O + N_2 = NO + N \quad (1)$$

$$N + O_2 = NO + O \quad (2)$$

$$N + OH = NO + H \quad (3)$$

Equation 4 gives then the NO formation rate via reactions in equations 1 to 3:

$$\frac{d[NO]}{dt} = k_1^+[O][N_2] + k_2^+[N][O_2] + k_3^+[N][OH] - k_1^-[NO][N] - k_2^-[NO][O] - k_3^-[NO][H] \quad (4)$$

[ ] in the equation 4 denotes species concentration in [kmol/m^2] and $k_i^+$and k_i^- represent the forward and reverse rate constants.

In the combustion engine, the post-flame gases NO formation always dominates the flame-front NO formation, due to the high combustion pressures, extremely thin flame reaction zone and rapid further compression after the combustion. *NOx* model therefore decouples the NO formation from combustion. Then, the equilibrium values at local pressure and equilibrium temperature approximate the concentrations of O, O_2, OH, H and N_2 [1].

$$\frac{d[NO]}{dt} = C_{NO_x} \frac{2R_1\left\{1-\left(\frac{[NO]}{[NO]_e}\right)^2\right\}}{1+\left(\frac{[NO]}{[NO]_e}\right)\left(\frac{R_1}{R_2+R_3}\right)} \quad (5)$$

Introduction of the equilibrium assumption and further evolution of the equation 4 yields the NO formation rate equation 5: $R_1 = k_1^+[O]_e[N_2]_e = k_1^-[NO]_e[N]_e$, with $[\ ]_e$ meaning the equilibrium concentration for the one-way equilibrium rate for the reaction in equation 1. Similarly, for the other two reactions $R_2 = k_2^+[N]_e[O_2]_e = k_2^-[NO]_e[O]_e$ and $R_3 = k_3^+[N]_e[OH]_e = k_1^-[NO]_e[H]_e$. Forward and reverse rate constants ($k_i^+$and k_i^- respectively) than change into one-way rate constants k_i (equations 6-8) [1].

$$k_1 = F_1 \cdot 7.6 \cdot 10^{10} \cdot e^{-38000 \cdot A_1/T_b} \quad (6)$$

$$k_2 = F_2 \cdot 6.4 \cdot 10^6 \cdot T_b \cdot e^{-3150 \cdot A_2/T_b} \quad (7)$$

$$k_3 = F_3 \cdot 4.1 \cdot 10^{10} \quad (8)$$

Equations 5-8 contain six calibration multipliers that we use to match the *NOx* model results with measurement from a specific ICE. These multipliers are following:

- NO_x Calibration Multiplier C_{NO_x}, that multiplies the overall NO production net rate (equation 5);
- N_2 Oxidation Rate Multiplier F_1 (equation 6);
- N_2 Oxidation Activation Energy Multiplier A_1 (equation 6);
- N Oxidation Rate Multiplier F_2 (equation 7);
- N Oxidation Activation Energy Multiplier A_2 (equation 7);
- OH Reduction Rate Multiplier F_3 (equation 8).

Regarding the temperature calculation, the *NOx* model uses a two-zone temperature calculation, to capture the maximum cylinder temperature more precisely and therefore enhance the NO_x formation prediction.

3. Experimental set-up and test matrix

For the calibration studies of the *NOx* model, we are using a set of experimental data originating from a steady-state measurement with a four-cylinder turbocharged SI engine. The combustion engine is rebuilt from a CI variant and fueled by natural gas with a usual average composition of the natural gas of: 98.39 [%vol] CH_4, 0.44 [%vol] C_2H_6, 0.26 [%vol] higher hydrocarbons and 0.84 [%vol] N_2. Table 1 summarizes the main parameters of the experimental engine.

Table 1. *Main parameters of the experimental ICE*

Bore	102 [mm]
Stroke	120 [mm]
Compression ratio	12
Configuration	R4
Valves per cylinder	4
IVO/IVC	342/595 [°CA aTDC] @ 0.1 mm lift
EVO/EVC	123/377 [°CA aTDC] @ 0.1 mm lift
Maximum Torque	600 Nm @ 1600-1800 RPM
Maximum Power	120 kW @ 2000 RPM

Our experimental ICE features a central mixer for metering and delivery of the gaseous fuel mixture downstream the compressor inlet. The fuel flow control is either automatic by a closed loop lambda control or manual. Conventional throttle – located downstream from the intercooler – controls the mixture inflow and a turbine with variable geometry controls the boost pressure. Experimental ICE is also equipped with a cooled low-pressure EGR system, with the EGR rate adjustment by a servo driven butterfly valve. High-energy ignition system has the possibility of the spark discharge angle adjustment or closed-loop CA50 control with the resolution of 0.25°CA.

A fully automated data acquisition system records the engine torque, engine speed, fuel flow, airflow and average temperatures in the intake and exhaust manifolds etc. A set of laboratory exhaust gas analyzers is used for continual analysis of the exhaust gas composition. Finally, a full three-pressure-analysis (TPA) is ensured by sensing the in-cylinder pressure with an uncooled piezoelectric transducer installed in the glow plug hole of the first cylinder and two piezo resistive pressure transducers sensing the intake and exhaust pressures. More details of the experimental set-up are summarized in [7, 8].

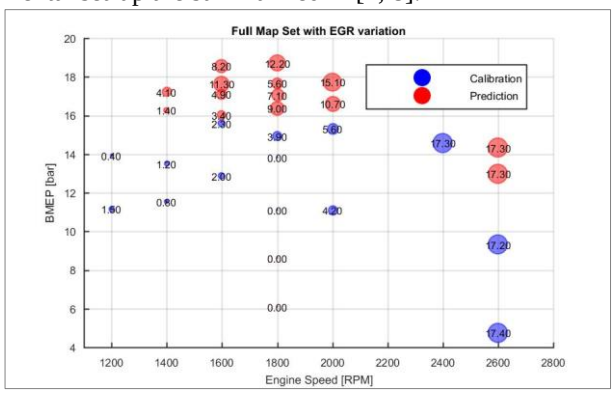

Fig. 1. *Test matrix with 30 operation points from the full map measurement set with stoichiometric mixture conditions and EGR ratio variation*

Figure 1 shows the reduced test matrix that contains 30 operation points in total: 14 operation points for the calibration (in blue), and 16 operation points for the prediction (in red). Details on the selection of the calibration and prediction points are given in the following chapter. The size of a circle (and a number) indicates the EGR content in [%].
This test matrix originates from 2007 steady-state measurement set of 83 operation points, representing the full engine map with the stoichiometric mixture and EGR ratio variations (BMEP 4.75-19.30 bar; 1200-2600 RPM).

4. Calibration procedure

Calibration procedure in general consists of two main steps:

1. Calibration of the basis TPA simulation model, that ensures a proper function of the thermodynamic model
2. Calibration of the NO_x model

The calibration can be either manual or as in our case fully automated using a genetic algorithm (GA) [9]. The determination of the optimal set of calibrated parameters implies the formulation of the objective functions for the specific calibration step. GA then minimizes these objective functions.
Result of a multi-criterial, multi-parameter optimization is a set of non-dominated solutions on a so-called Pareto Frontier. To obtain a single optimal solution from the Pareto set, we use a criterial function:

$$F_{crit} = \sum_{i=1}^{k} \alpha_k \frac{X_k}{X_{k,max}} \tag{9}$$

The fraction $X_k/X_{k,max}$ represents a normalization, so that different objective functions X_k can be combined into a single equation; $X_{k,max}$ is a maximum value from all Pareto set solutions, for the respective objective function X_k; and α_k is a criterial function weight factor.

4.1. Basis TPA model calibration

Basis TPA model calibration corrects some model uncertainties and possible measurement errors. We apply the same TPA model calibration as in our study on the predictive capabilities of a phenomenological combustion model [10], since we use the same test matrix for both studies.
Chapter 4.1 of [10] gives more information regarding the basis TPA model calibration parameters, objective functions and selected optimal TPA model settings.

4.2. NO_x emission model

The calibration parameters for the subsequent NO_x emission model calibration are the six NO_x model multipliers, which we already summed-up at the end of Chapter 2.
We calculate the error of the NO_x model as a difference between the measurement and simulation NO_x concentration, testing two different options: either a simple difference in absolute value (equation 10) or a percentage error in absolute value (equation 11).

$$\Delta NO_x = \left| NO_{x_{meas}} - NO_{x_{sim}} \right| \tag{10}$$

$$\%NO_x = \left| \frac{NO_{x_{meas}} - NO_{x_{sim}}}{NO_{x_{meas}}} \right| \tag{11}$$

NO_x model outputs the ΔNO_x or $\%NO_x$ errors for all operation points. The maxima and the average value serve as the objective functions, leading into two objective functions X_k and equal weight factors α_k (Table 2).

Table 2. *Objective functions and weight factors for the NO_x model calibration*

Objective function X_k	Weight factor α_k
Average ΔNO_x/$\%NO_x$	0.5
Maximum ΔNO_x/$\%NO_x$	0.5

4.3. NO_x model calibration studies

After the calibration of the basis TPA model, we have conducted following studies on the NO_x model calibration:

- Study of NO_x model's calibration on the ICE full map;
- Study of NO_x model's predictive capability, using both the calibration and prediction points from the test matrix.

4.2.1. NO_x model full map calibration

The full test matrix (Figure 1) contains 30 operation points. We have taken in total 21 operation points covering the whole ICE map for the full map calibration. GA than calibrated the NO_x model on this extended set.
We repeated the calibration using the objective functions first derived from ΔNO_x error and second from the $\%NO_x$ error.

4.2.2. NO_x model predictive capability

For the second study, we have chosen 14 points from the full test matrix as calibration points and the remainder 16 as prediction points.
The calibration points represent medium ICE loads; low to medium speeds and EGR rates 0-5.6%. Only three calibration points contain high EGR rate of 17% and high ICE speeds (2400 and 2600 RPM).
The prediction points then cover low load/high load parts of the map, generally with high EGR rates (except for two low load points @ 1800 RPM with 0% EGR rate).
GA calibrated the NO_x model on the calibration points and then we evaluated its performance also on the prediction points.
Even in this case we repeated the calibration with both objective functions: derived from ΔNO_x error and $\%NO_x$ error.

5. Results and discussion

5.1. NO_x model full map calibration results

On the full map calibration study, GA calibrated the NO_x model on the extended set of 21 operation points, using different objective functions (ΔNO_x errors and $\%NO_x$ errors). Figure 2 shows resulting Pareto Frontiers of these calibrations.

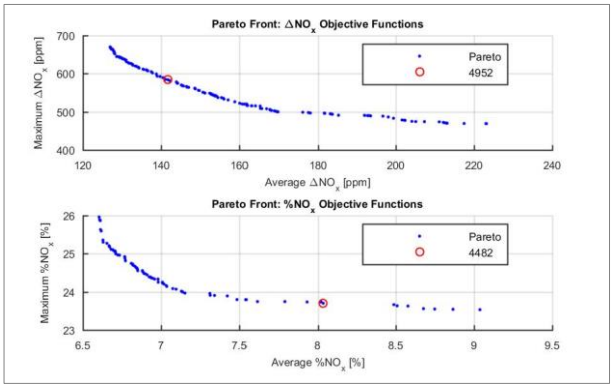

Fig. 2. *Pareto Frontiers with the optimum points for the NO_x emission model (full map calibration)*

We have than used a criterial function (equation 9; Table 2 with weight factors α_k) to obtain the final optimal solutions (solutions 4952 and 4482). Table 3 than sums-up the NO_x model parameter values for both optimal solutions.

Table 3. *Optimal values of the calibration parameters for the NO_x emission model (full map calibration)*

Parameter	ΔNO_x Objective functions (#4952)	$\%NO_x$ Objective functions (#4482)
C_{NO_x}	0.435	0.412
F_1	0.182	0.175
A_1	0.841	0.825
F_2	2.639	1.517
A_2	0.107	1.033
F_3	0.354	0.384

Table 4 covers the average and maximum errors (in absolute value!) for both calibrations. Calibration with $\%NO_x$ derived objective functions achieves better [%] results, as can be expected. The ΔNO_x calibration performs better only in maximum difference [ppm] result.

Table 4. *Average and maximum NO_x formation errors for (full map calibration)*

Objective functions	Average error	Maximum error
ΔNO_x	154.6 [ppm]	537.3 [ppm]
	9.5 [%]	29.4 [%]
$\%NO_x$	131.2 [ppm]	643.2 [ppm]
	6.9 [%]	24.6 [%]

Figures 3 and 4 than show a graphical representation of the results in Table 4: operation points where the NO_x model overestimates the NO_x concentration are in blue, underestimated points are in red.

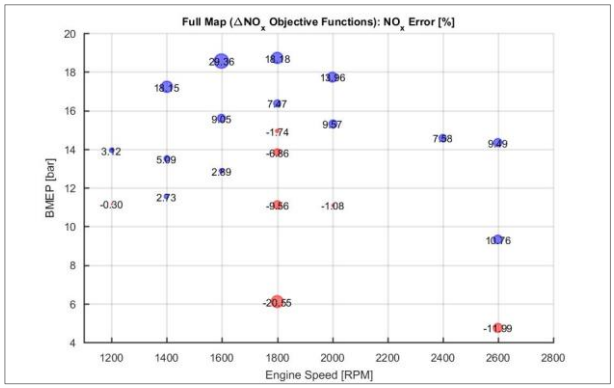

Fig. 3. *NO_x percentage errors (experimental versus simulation values) for the ΔNO_x objective functions (full map calibration)*

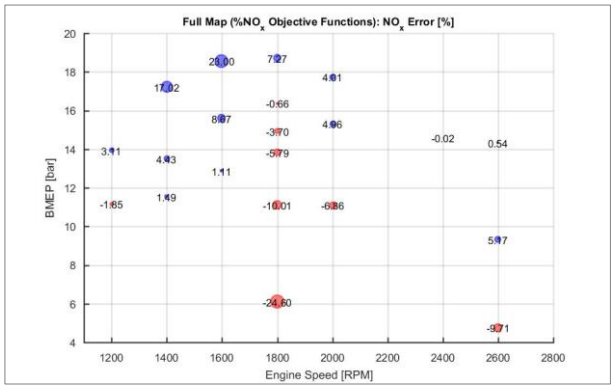

Fig. 4. *NO_x percentage errors (experimental versus simulation values) for the $\%NO_x$ objective functions (full map calibration)*

Full map calibration of the NO_x model confirms the results from [4], where the authors state, that the EZM models can be in error up to 40%. Our calibrations show errors up to 25-30%, depending on the set of objective functions.

5.2. NO_x model predictive capability results

In this study the GA calibrated the NO_x model on a calibration set, using again the different objective functions. Figure 5 shows resulting Pareto Frontiers.

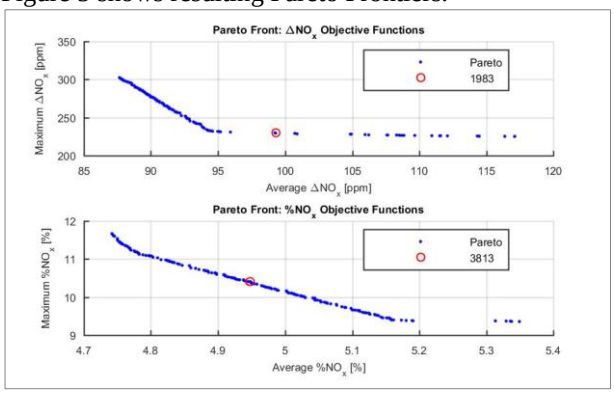

Fig. 5. *Pareto Frontiers with the optimum points for the NO_x emission model (study of the predictive ability)*

A criterial function determined the final optimal solutions (1983 and 3813). NO_x model parameter values for both optimal solutions are than summed-up in Table 5.

Table 5. *Optimal values of the calibration parameters for the NO_x emission model (study of the predictive ability)*

Parameter	**ΔNO_x Objective functions** (#1983)	**$\%NO_x$ Objective functions** (#3813)
C_{NO_x}	0.428	0.419
F_1	0.135	0.153
A_1	0.821	0.820
F_2	2.849	2.539
A_2	0.844	1.024
F_3	0.060	0.045

After the model calibration, we used the optimal NO_x model settings to simulate also the prediction set.
Table 6 contains the average and maximum errors (again in absolute value) for both the calibration and prediction simulations. Note, that the performance of both optimal sets is very similar, especially for the average error.

Table 6. *Average and maximum NO_x formation errors for (study of the predictive ability)*

Objective functions	**Average error** (calibration/prediction)	**Maximum error** (calibration/prediction)
ΔNO_x	94.6/220.1 [ppm]	232.0/607.3 [ppm]
	5.3/11.6 [%]	14.9/26.6 [%]
$\%NO_x$	93.8/214.0 [ppm]	247.4/626.2 [ppm]
	5.2/11.4 [%]	9.4/23.9 [%]

Figures 6 and 7 than represent graphically the results of Table 6: negative error is in red, positive error in blue.

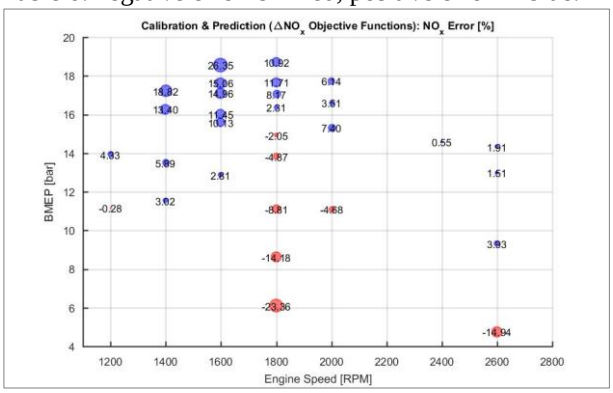

Fig. 6. *NO_x percentage errors (experimental versus simulation values) for the ΔNO_x objective functions (study of the predictive ability)*

Similar trend as in full map calibration is present: model performs very well in medium loads and medium EGR range. But the points with higher (or lower) load/EGR display higher errors in general (note, that in our study high load operation points generally have high EGR content). This could be further reduced by the introduction of the functional dependencies of some of the NO_x model parameters (especially the main calibration parameter C_{NO_x}) on the EGR content or ICE load.

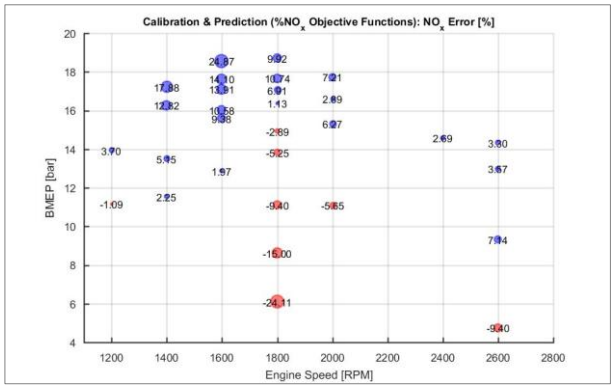

Fig. 7. *NO_x percentage errors (experimental versus simulation values) for the $\%NO_x$ objective functions (study of the predictive ability)*

Maximum and average errors in this study of NO_x model's predictive abilities are even slightly lower than in the full map calibration. Therefore, we can conclude that the model is capable of prediction. But the predictive ability must be further tested on an extended set, also with non-stoichiometric data.

6. Conclusions

We have calibrated a NO_x emission formation model, based on an extended Zel'dovich mechanism principle with six calibration parameters.
First, we did a detailed calibration of the model using genetic algorithm on a full ICE operation map and then tested its predictive ability. For both studies we have also tested different calibration approaches: either using objective functions derived from a simple difference between measured and simulated NO_x concentration or using objective functions derived from a percentage difference.

The full model calibration study shows that:

- Agreement with the experimental data can be achieved in a range of error up to 30%, which is slightly better compared to the literature [4];
- Model performs very well in a range of low to medium EGR content and in medium loads (maximum error up to 10%);
- Introduction of the functional dependencies of some of the emission model parameters on the EGR content or ICE load should improve the results.

The results from the study of the predictive abilities of the emission formation model show:

- Model performs very well inside the calibration range (maximum error up to 10%, average error lower than for full map calibration);
- Outside its calibration range the results reach the same quality compared to full map calibration;
- Therefore, the model has a predictive ability. Nevertheless, this must be further tested on an extended set, with e.g. non-stoichiometric mixture conditions.

Finally, testing of different sets of objective functions show that:

- The difference between two approaches (simple difference and percentage error) is small;
- Although, the calibrations with percentage error derived objective functions show slightly better results.

In conclusion, our work confirms the performance of different EZM models in general. However, the addition of model calibration multipliers allows for the further error reduction and model adaption for different ICE.
Our future development will focus on an extended measurement data set from the natural gas ICE, with non-stoichiometric mixture conditions. We will also study the possible error reduction by the introduction of functional dependencies of some model parameters (especially the main calibration parameter) on the EGR content or ICE load.

Acknowledgements

This work was supported by the Grant Agency of the Czech Technical University in Prague, grant No. SGS16/213/OHK2/3T/12.

List of abbreviations

0D	Zero-Dimensional
1D	One-Dimensional
3D	Three-Dimensional
A/F	Air to Fuel ratio
BMEP	Brake Mean Effective Pressure
CA	Crank Angle
CAE	Computer-aided Engineering
CFD	Computational Fluid Dynamics
EGR	Exhaust Gas Recirculation
EVC	Exhaust Valve Close
EVO	Exhaust Valve Open
EZM	Zel'dovich Mechanism
GA	Genetic Algorithm
ICE	Internal Combustion Engine
IVC	Intake Valve Close
IVO	Intake Valve Open
LHV	Lower Heating Value
NO	Nitric Oxide
NO_2	Nitrogen Dioxide
NO_x	Nitrogen Oxides (generic term)
SEZM	Super-Extended Zel'dovich Mechanism
SI	Spark Ignition
TDC	Top Dead Center
TPA	Three-Pressure-Analysis

List of notations

A_1	N_2 Oxidation Activation Energy Multiplier (-)
A_2	N Oxidation Activation Energy Multiplier (-)
C_{NO_x}	NO_x Calibration Multiplier (-)
F_{crit}	Criterial Function (-)
F_1	N_2 Oxidation Rate Multiplier (-)
F_2	N Oxidation Rate Multiplier (-)
F_3	OH Reduction Rate Multiplier (-)

k_1 N_2 Oxidation Rate Constant ($m^3 \cdot kmol^{-1} \cdot sec^{-1}$)
k_2 N Oxidation Rate Constant ($m^3 \cdot kmol^{-1} \cdot sec^{-1}$)
k_3 OH Reduction Rate Constant ($m^3 \cdot kmol^{-1} \cdot sec^{-1}$)
p Pressure (Pa)
T_b Burned sub-zone Temperature (K)
X_k Objective Function (-)
α_k Criterial Function Weight Factor (-)

References

[1] Heywood, J. B. (1988). Internal Combustion Engine Fundamentals, McGraw-Hill, New York, ISBN 0-07-028637-X

[2] Karaky, H., Mauviot, G., Tauzia, X., Maiboom, A. (2015). Development and Validation of a New Zero-Dimensional Semi-Physical NOx Emission Model for a D.I. Diesel Engine Using Simulated Combustion Process, **SAE Int. J. Engines**, Vol. **8**, No. **4**, doi:10.4271/2015-01-1746

[3] Miller, R., Davis, G., Lavoie, G., Newman, C., Gardner, T. (1998). A Super-Extended Zel'dovich Mechanism for No_x Modeling and Engine Calibration, **SAE Technical Paper** 980781, doi:10.4271/980781

[4] Miller, R., Russ, S., Weaver, C., Kaiser, E., Newman, C., Davis, G., Lavoie, G. (1998). Comparison of Analytically and Experimentally Obtained Residual Fractions and NO_x Emissions in Spark-Ignited Engines, **SAE Technical Paper** 982562, doi:10.4271/982562

[5] Hvězda, J. (2014). Multi-Zone Models of Combustion and Heat Transfer Processes in SI Engine. **SAE Technical Paper** 2014-01-1067, doi:10.4271/2014-01-1067

[6] GT-POWER Engine Performance Application Manual. [Manual] Westmont: Gamma Technologies, Inc., 2015

[7] Škarohlíd, M. (2010). Modeling of Influence of Biogas Fuel Composition on Parameters of Automotive Engines, **SAE Technical Paper** 2010-01-0542, doi:10.4271/2010-01-0542

[8] Vávra, J., Takáts, M., Klír, V., Škarohlíd, M. (2012). Influence of Natural Gas Composition on Turbocharged Stoichiometric SI Engine Performance, **SAE Technical Paper** 2012-01-1647, doi:10.4271/2012-01-1647

[9] modeFRONTIER – Multi-Objective Design Environment, version 4.4.3. [CD-ROM], 2012

[10] Toman, R., Macek, J. (2017). Evaluation of the Predictive Capabilities of a Phenomenological Combustion Model for Natural Gas SI Engine, **Journal of MECCA**, Vol. **15**, No. **2**, doi:10.1515/mecdc-2017-0007